Kinematic theory of ballistic electron emission spectroscopy of silicon–silicide interfaces

M. D. Stiles
National Institute of Standards and Technology, Gaithersburg, Maryland 20899

D. R. Hamann
AT&T Bell Laboratories, Murray Hill, New Jersey 07974

(Received 29 January 1991; accepted 12 April 1991)

The electronic structure of the materials being measured has a strong effect on the spectroscopy of the interface between them measured by ballistic electron emission microscopy (BEEM). Specific calculations for $CoSi_2/Si(111)$ and $NiSi_2/Si(111)$ based on the calculated band structures of the materials illustrate some of the observable effects due to band structures, particularly of the overlayer. The BEEM spectra for $CoSi_2/Si(111)$ show a delayed onset due to a mismatch of the states near the conduction band minimum in the Si. The spectra for $NiSi_2/Si(111)$ show structure due to a decrease in the density of states in the $NiSi_2$ at ~ 1.8 eV above the Fermi level.

Spectroscopic studies of $CoSi_2/Si(111)$ and $NiSi_2/Si(111)$ interfaces using ballistic electron emission microscopy (BEEM) provide a test of both our understanding of the spectroscopy itself and of the electron transmission process across interfaces. The silicides are quite closely lattice matched to silicon and share common (111) planes so it is possible to grow high quality interfaces.[1,2] Since the interfaces are atomically abrupt and coherent, it should be possible to calculate accurate BEEM spectra that do not depend on assumptions like a free electron approximation for the metal overlayer or an effective mass approximation for the semiconductor substrate.

An interesting feature of the $CoSi_2/Si(111)$ interface is that there is a projected band gap in the $CoSi_2$ at the energy and parallel wave vector corresponding to the conduction band minimum in Si.[3] This implies that for some energy range above the Schottky barrier, the ballistic transmission probability across the interface will be zero, which will degrade the performance of metal-base transistors based on these materials. The original interest in these systems was stimulated by the expectation that they would make good transistors[4] because of the high quality interfaces that could be grown. The best transistors that were made performed quite poorly, consistent with the prediction of an absence of ballistic transmission at good interfaces, but the exact cause was not pinned down. The ability of BEEM spectroscopy to vary the distribution of electrons incident on the interface in a more controlled manner gives the possibility of directly observing the predicted energy gap.

Depending on growth conditions, it is possible to grow two types of $NiSi_2/Si(111)$ interfaces, in some cases both on the same substrate. Thus, it should be possible to compare the BEEM spectra for the two interfaces while holding other aspects of the experiment constant. The interfaces are predicted to have different transmission properties[5] allowing a test of our understanding of these systems.

In a BEEM experiment, a scanning tunneling microscope (STM) tip is held over the metal overlayer, with a voltage applied between the tip and the overlayer, and the overlayer and substrate held at the same voltage. Electrons are injected into the overlayer, some of which travel ballistically across the overlayer and are incident on the Schottky barrier between the overlayer and the substrate. Independent electrical contact is made to the substrate and the current between the tip and the substrate is measured. The collector current as a function of tip voltage can be used to infer properties of the interface, like the Schottky barrier height, and the behavior of the transmission across the interface. By scanning the tip while measuring the collector current, local variations in the Schottky barrier due to changes in the interface can be imaged.

The collector current in a BEEM experiment is equal to the integral of the flux distribution incident on the interface between the overlayer and the substrate times the probability that an electron in each state will be transmitted across the interface,

$$I_c(V,d) = e \sum_n \int_{\mathrm{BZ}} \frac{d^3k}{(2\pi)^3} v_z(n,\mathbf{k}) \rho_I(n,\mathbf{k},V,d) T(n,\mathbf{k}). \tag{1}$$

Here, V is the applied voltage, d is the tip-sample separation, n is a band index, BZ is the bulk Brillouin zone of the overlayer, $\mathbf{k}$ is a wave vector, v_z is the group velocity, ρ_I is the distribution of electrons incident on the interface, and T is the transmission probability across the interface. Since the group velocity is the wave vector derivative of the energy, the above expression can be rewritten,

$$I_c(V,d) = e \int dE \int_{\mathrm{IBZ}} \frac{d^2K}{(2\pi)^2} \sum_{n'} \times \rho_I(n',E,\mathbf{K},V,d) T(n',E,\mathbf{K}), \tag{2}$$

where IBZ is the interface Brillouin zone determine by the common interface lattice net of the two materials, $\mathbf{K}$ is a wave vector in the interface Brillouin zone, and n' references all the states in the overlayer with a given E and $\mathbf{K}$.

In this paper we discuss how the band structures of the materials affect the BEEM spectra of the interfaces, and use some approximate models of the incident distribution, ρ_I, to compute the collector current.

Energy is conserved when electrons transmit across the interface and, for coherent interfaces (those with interface

 0734-211X/91/042394-05$01.00

lattice nets for each material that match) the crystal momentum parallel to the interface is conserved. These two conservation principles constrain the transmission such that if there is no state in the substrate with the same E and $\mathbf{K}$, which we will refer to as a corresponding state, there can be no ballistic transmission. Below we use a model, which we will refer to as a kinematic model, K_1, in which all kinematically allowed transmission probabilities are set to 1. Note that there can be any number of corresponding states since at a general energy several different bands are involved, and each band can have multiple extrema.

It is possible to improve on this kinematic model with minimal effort by using the property that the total transmission into a given state summed over incident states is <1. This constrains the transmission probability when there are more states in the overlayer than there are in the substrate at a given E and $\mathbf{K}$. If there are N states in the overlayer and M in the substrate, then the maximum average transmission probability for a state in the overlayer will be M/N. Using these constraints, we construct another kinematic model for the transmission, K_2, in which the transmission probability for a state in the overlayer is 1 if there are more states in the substrate than in the overlayer, and M/N otherwise.

Both of the kinematic models discussed above only depend on the band structures of the two materials and the Schottky barrier of the interface. A full dynamical calculation,[6] D, also accounts for the atomic scale details of the states in each material and of the potential at the interface. The kinematic models give an upper bound for the transmission across the interfaces and determine the general shapes of the spectra. However, to correctly determine the detailed shapes and the amplitudes of the spectra it is necessary to include the dynamic effects in the transmission probabilities.

To compute the collector current using the above transmission models, the distribution of electrons incident on the interface is needed. Unfortunately, this is much more complicated to calculate from first principles than the transmission across the interface. We consider a simple model and discuss the results below. The first process determining the incident distribution is the tunneling distribution of current injected into the overlayer from the tip. The gross features of this distribution are straightforward to treat, but any state specific details depend on unknown details of the tip and surface electronic structure. Previous treatments of BEEM[7,8,9] have computed the tunneling probability with the planar barrier tunneling model, which is essentially a Wentzel–Kramers–Brillouin (WKB) approximation. The tunneling probability depends on the energy minus the kinetic energy of motion parallel to the interface, $E_\perp = E - K^2/2m$. (We use atomic units: $\hbar$ is 1, masses are in electron masses, distances are in bohr radii, and energies are in hartrees.) In addition, we make a correction for the applied voltage, V, across the barrier of height, V_b,

$$t(E_\perp,V,d) = \exp\left\{-2d\left[2m(V_b-E_\perp)\right]^{1/2} \times\left[\frac{1-\left(1-\frac{V}{V_b-E_\perp}\right)^{3/2}}{\frac{3}{2}\frac{V}{V_b-E_\perp}}\right]\right\}. \quad (3)$$

With this model the tip current is

$$I_t(V) = e\int dE \int_{\mathrm{IBZ}} \frac{d^2K}{(2\pi)^2}\sum_{n'}\rho_t(n',E,\mathbf{K},V,d), \quad (4)$$

where $\rho_t(n',E,\mathbf{K},V,d) = \alpha t(E_\perp,V,d)$ is the distribution of tip current. The scale factor α is included since this model otherwise neglects any effects due to the density of states in the tip, inelastic tunneling, and variation in the tunneling amplitudes due to the atomic scale details of the wave functions at the overlayer surface. Note that the electron distributions used in this calculation are normalized such that their integral leads to the total currents rather than current densities.

In addition to the simplified model for the tunneling, we also ignore scattering in the overlayer and approximate ρ_I by ρ_t. In addition, we ignore scattering in the substrate[10] by assuming that the transmission probability depends only on the reflection due to wave function mismatch. We note that since the Schottky barrier energy is more than 20 times the thermal energy at room temperature, and there is no voltage applied between the overlayer and the substrate, that thermal excitation of electrons to energies at which they can transmit over the barrier is negligible. While scattering could have a significant effect on the measured collector current, we focus on the transmission across the interface because it is the main experimental interest. By comparing calculations of BEEM spectra with measured ones, it may be possible to infer the effect of some of the processes we ignore in these calculations.

In order to examine the threshold behavior of the transmission across the $CoSi_2$/Si(111) interface it is necessary to have a very fine mesh for both the parallel wave vectors and the energy. This situation would make the calculation prohibitive if all of the points were calculated from a bulk band structure; instead we calculate a small set, 48, of special k-points in the irreducible wedge of the bulk Brillouin zone and make a fit to the band structures that allows us to easily calculate the bands at any wave vector. We fit the bands to a set of plane waves taken from a symmetrized set of real space lattice vectors in much the same way that a potential in real space is fit to reciprocal space lattice vectors. Although this fit works well for our purpose it is not perfect because it is impossible to fit cusps and curve crossings with any finite set of plane waves.

Figure 1 shows the Si and $CoSi_2$ bands along some high symmetry lines of the bulk Brillouin zone. The solid points are the energy bands at some of the wave vectors calculated by the linearized augmented plane wave (LAPW) implementation[3,11] of the local density approximation (LDA) which we use to calculate the electronic structure. The solid lines are the fit that is used to calculate the BEEM spectra discussed below. The fit uses 22 sets of symmetry related lattice vectors, a total of 459 plane waves. The agreement with the first principles calculation is not perfect, but is good enough for the properties we are calculating in which we integrate over much of phase space. We have tested the fit by varying the number of plane waves, and special k-point samples, and do not find significant differences in the BEEM spectra.

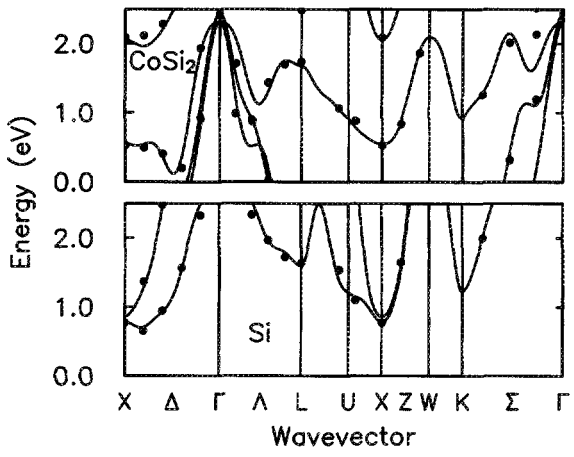

FIG. 1. Bulk band structures for Si and $CoSi_2$. The energy bands relevant to this calculation are shown plotted along a series of high symmetry lines in the bulk Brillouin zone for the two materials. ● are the points from the self-consistent calculation of the band structures. — are the fits to these bands as described in the text.

Using this fit to the bands of both materials, we calculate the bands on a finer mesh of wave vectors. At each wave vector parallel (we use 217) to the interface we find, as a function of energy, the number of states in each material. A subset of this calculation is shown in Fig. 2. This figure shows part of the distribution of states in both materials in terms of their energy and parallel wave vector in the interface Brillouin zone. Since the interface Brillouin zone is highly symmetric, only an irreducible wedge of it is shown; the rest of the hexagonal interface Brillouin zone is given by rotations of the wedge around the origin $\bar{\Gamma}$ and reflections around the edges that go through the origin. At each energy that is shown a circle is drawn at each parallel wave vector at which there is a state in the $CoSi_2$, and a plus at each parallel wave vector at which there is a state in the Si. When there is a state in both materials, the two symbols combine to form a filled circle.

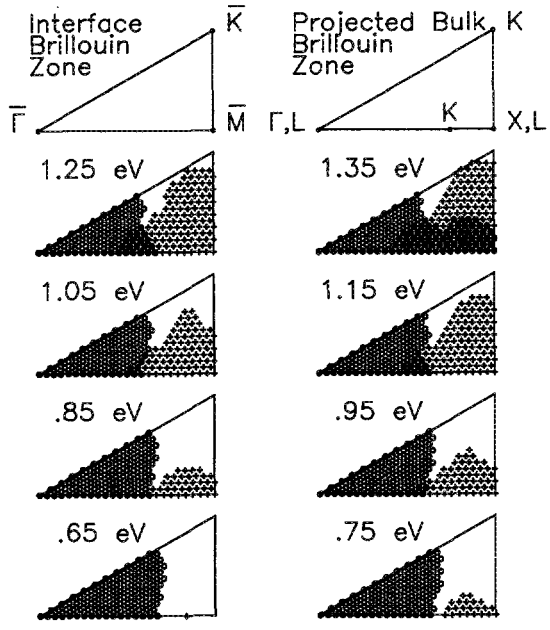

FIG. 2. Phase space for electron transmission through a $CoSi_2$/Si(111) interface. The panels show the irreducible wedge of the interface Brillouin zone of both the $CoSi_2$ and the Si. At each parallel wave vector used in the calculation there is an open circle if there is at least one state at that energy in the $CoSi_2$ and a plus if there is at least one state in the Si. If there is a state in both the open circles fill in and become closed circles.

This figure shows the origin of the delay in the onset of transmission above the Schottky barrier. At energies just above the Schottky barrier, the $CoSi_2$ does not have states in the same part of phase space as the Si conduction band minimum. Thus, all of the flux incident on the interface from the $CoSi_2$ is carried by states that do not have corresponding states in the Si and hence cannot transmit ballistically across the interface. As the energy increases the area in reciprocal space in which both materials have states increases, and at ~0.2 eV above the threshold there are states that can couple. Note that it is even higher in energy before there are states in the $CoSi_2$ that correspond to the Si conduction band minimum.

Using these states, the kinematical models for the transmission, and the simple model for the incident distribution, we calculate the constant height BEEM spectra seen in Fig. 3. The spectra has been calculated using the simple model discussed above, and is plotted as the ratio of the collector current to the tip current to divide out the large, roughly exponential increase in the tunneling current. Taking the ratio has the additional virtue of removing some of the uncertainty in the tunneling probability. The ratio of currents is very similar to the collector current measured in constant current mode, but the incident distribution varies more strongly with voltage in the latter case. Taking the ratio of the derivative of both currents with respect to voltage[6] removes even more of the uncertainty. The delay in transmission above the Schottky barrier height is clearly seen. There is a fairly large difference in the two kinematical models primarily due to there being more states in the $CoSi_2$ than in the Si at the parallel wave vectors where they overlap. The detailed amplitude of the BEEM spectra will depend on the transmission probabilities which have not been calculated for this interface. Kaiser *et al.*[12] have measured the BEEM spectrum for $CoSi_2$/Si(111) and found a delayed onset of ~0.2 V, quite close to our calculated value. They also ob-

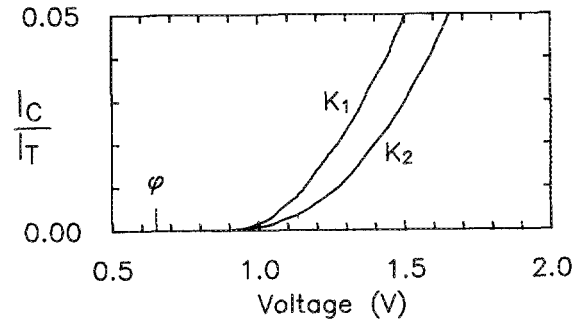

FIG. 3. BEEM current for $CoSi_2$/Si(111) interfaces. The BEEM current is plotted as a function of tip-sample voltage for two models of the transmission, K_1 and K_2, as discussed in the text. The Schottky barrier ϕ is labeled.

serve a second apparent threshold at ~1.1 V that is seen in some theoretical calculations depending on the details of the model for the barrier.

We have carried out full dynamical calculations for $NiSi_2/Si(111)$.[5,6] Comparing those results with kinematic calculations for these interfaces can give an indication of the importance of dynamical effects. In Fig. 4 we show the transmission probabilities, calculated using all three models, averaged over parallel wave vector and states. There is a fair amount of noise in the curves due to the discrete parallel wave vector sampling. Because the dynamic calculation is much more time consuming we use a much smaller sample (here 30) of parallel wave vectors. We have done strictly kinematical calculations like those done for the $CoSi_2/Si(111)$ interface and find no differences except for numerical noise. The curves labeled K_1, computed using the simple kinematic model show the expected linear increase close to threshold (within the noise) that is due to the increasing area in reciprocal space of allowed states in the Si. Above 1.8 eV there are states in the Si at almost all parallel wave vectors, so the average kinematic transmission probability is close to 1. The curves labeled K_2 lie significantly below the K_1 curves, particularly at the highest energies, showing that that there tend to be more corresponding states in the $NiSi_2$ than the Si. The number of states in the $NiSi_2$ averaged over the parallel wave vector is shown in the top panel of Fig. 4; in a free electron model, this curve would be unity over the whole energy range. The dip seen around 1.8 eV leads to features in the BEEM current as is seen below. The full transmission probability[6] is used to compute the curves labeled D; these curves show the difference in transmission for the two interfaces discussed above; this difference is not seen in the kinematical models. Just above threshold, the A-type transmission is a much higher fraction of the kinematic transmission than is the B-type. This difference disappears around 0.4 eV above threshold, and then returns at higher energies although not as dramatically. Note that the kinematical model K_2 includes the decrease in transmission above 1.8 eV that is missing in the model K_1.

Using these transmission probabilities we calculate the BEEM spectra shown in Fig. 5. The spectra show much structure due to the tunneling distribution being strongly focused toward the zone center where the transmission probability is zero for most of the energies that contribute to this figure. As states become available in the Si close to the zone center (around 1.8 eV for the A-type interface) the collector current increases rapidly. At slightly lower energies there is a decrease in the density of states in the $NiSi_2$ which leads to the leveling off below the rapid increase in both spectra. While the transmission probability is increasing for these energies, the decrease in the density of states forces the tunneling current to flow through lower energy states where the transmission probability is not as high.

Comparing the kinematical and the dynamical calculations for the two interfaces indicates how much of the difference between their BEEM spectra is due to the different Schottky barriers, and how much is due to the different transmission across the two interfaces. The differences in the structure found in these curves is seen to be due to the difference in the band lineups, but the difference in the magnitude of the BEEM current is due to the differences in the transmission probabilities. In earlier calculations[5] we showed

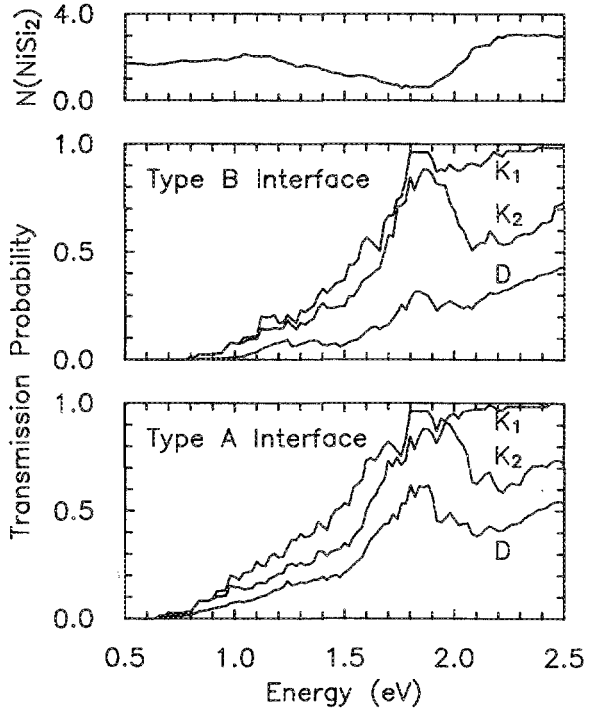

FIG. 4. Average transmission probability for electrons through $NiSi_2/Si(111)$ interfaces. The bottom (middle) panel shows the transmission probabilities for a type-A (type-B) interface averaged over parallel wave vector as a function of the energy above the $NiSi_2$ Fermi level. The curves D are the full dynamical results, the curves K_1 and K_2 are two kinematical models discussed in the text. The top panel shows the number of states in the $NiSi_2$ averaged over the parallel wave vector.

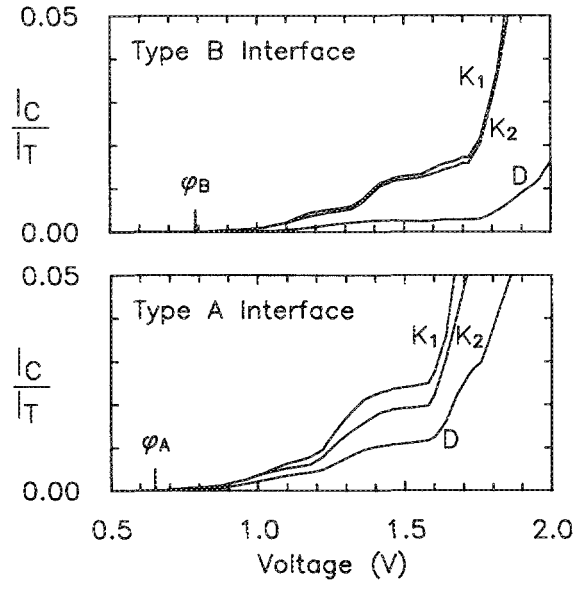

FIG. 5. BEEM current for $NiSi_2/Si(111)$ interfaces. The BEEM current is plotted as a function of tip-sample voltage for two models of the transmission, K_1 and K_2, as discussed in the text and for the full dynamical results, D. The Schottky barrier ϕ is labeled for each interface.

that the difference in the transmission probability is not due to the difference in the band lineups. Artificially changing the Schottky barrier of one interface type to that of the other did not appreciably affect the transmission probability. These spectra are strongly sensitive to the tip-sample separation, which is not well known so that direct comparison with experimental results[8,13] is difficult.

We have shown how the band structures of materials can effect BEEM spectra. The transmission across the $CoSi_2/Si(111)$ interface is expected to be zero for a range above threshold due to the mismatch in reciprocal space of the states in the two materials. The $NiSi_2/Si(111)$ interfaces are expected to show structure due to a decrease in the $NiSi_2$ density of states. They are are expected to show a significant difference between the two interfaces, but this is due to dynamical rather than kinematical effects.

[1] S. Saitch, H. Ishiwara, and S. Furukawa, Appl. Phys. Lett. **37**, 203 (1980); J. C. Bean and J. M. Poate, *ibid.* **37**, 643 (1980).
[2] R. T. Tung, J. M. Gibson, and J. M. Poate, Phys. Rev. Lett. **50**, 429 (1983); D. Cherns, G. R. Anstis, J. L. Hutchinson, and J. C. H. Spence, Philos. Mag. A **46**, 849 (1982); E. Vlieg, A. E. M. J. Fischer, J. F. van der Veen, B. N. Dev, and G. Materlik, Surf. Sci. **178**, 36 (1986); E. J. van Loenen, J. W. M. Frenken, J. F. van der Veen, and S. Valeri, Phys. Rev. Lett. **54**, 827 (1985).
[3] L. F. Mattheiss and D. R. Hamann, Phys. Rev. B **37**, 10 623 (1988).
[4] A. F. J. Levi, R. T. Tung, J. L. Batstone, and M. Anziowar, Proc. Mater. Res. Symp. Soc. Proc. **107**, 259 (1988).
[5] M. D. Stiles and D. R. Hamann, Phys. Rev. B **40**, 1349 (1989).
[6] M. D. Stiles and D. R. Hamann (unpublished).
[7] W. J. Kaiser and L. D. Bell, Phys. Rev. Lett. **60**, 1406, (1988); L. D. Bell and W. J. Kaiser, *ibid.* **61**, 2368 (1988); L. D. Bell, M. H. Hecht, W. J. Kaiser, and L. C. Davis, *ibid.* **64**, 2679 (1990); M. H. Hecht, L. D. Bell, and W. J. Kaiser, Appl. Surf. Sci. **41**, 17 (1989); M. H. Hecht, L. D. Bell, W. J. Kaiser, and L. C. Davis, Phys. Rev. B **42**, 7663 (1990).
[8] A. Fernandez, H. D. Hallen, T. Huang, R. A. Buhrman, and J. Silcox, J. Vac. Sci. Technol. B **9**, 590 (1991); A. Fernandez, H. D. Hallen, T. Huang, R. A. Buhrman, and J. Silcox (unpublished); H. D. Hallen, A. Fernandez, T. Huang, R. A. Buhrman, and J. Silcox, (unpublished).
[9] M. Prietsch and R. Ludeke, Phys. Rev. Lett. **66**, 2511 (1991); R. Ludeke and M. Prietsch, (unpublished).
[10] L. J. Schowalter and E. Y. Lee, Phys. Rev. B **43**, 9308 (1991); E. Y. Lee and L. J. Schowalter, (unpublished).
[11] Y. J. Chabal, D. R. Hamann, J. E. Rowe, and M. Schlüter, Phys. Rev. B **25**, 7598 (1982); D. M. Bylander, L. Kleinman, K. Mednick, and W. R. Grise, *ibid.* **26**, 6379 (1982).
[12] W. J. Kaiser, M. H. Heckt, R. W. Fathauer, L. D. Bell, E. Y. Lee, and L. C. Davis (unpublished).
[13] Y. Hasagawa, Y. Kuk, T. T. Tung, P. J. Silverman, and T. Sakurai, J. Vac. Sci. Technol. B **9**, 578 (1991); Y. Hasagawa and Y. Kuk (unpublished).